DNA Analysis

DOI: 10.1002/anie.200901887

Gold-Nanoparticle-Based Multicolor Nanobeacons for Sequence-Specific DNA Analysis**

Shiping Song, Zhiqiang Liang, Juan Zhang, Lihua Wang, Genxi Li, and Chunhai Fan**

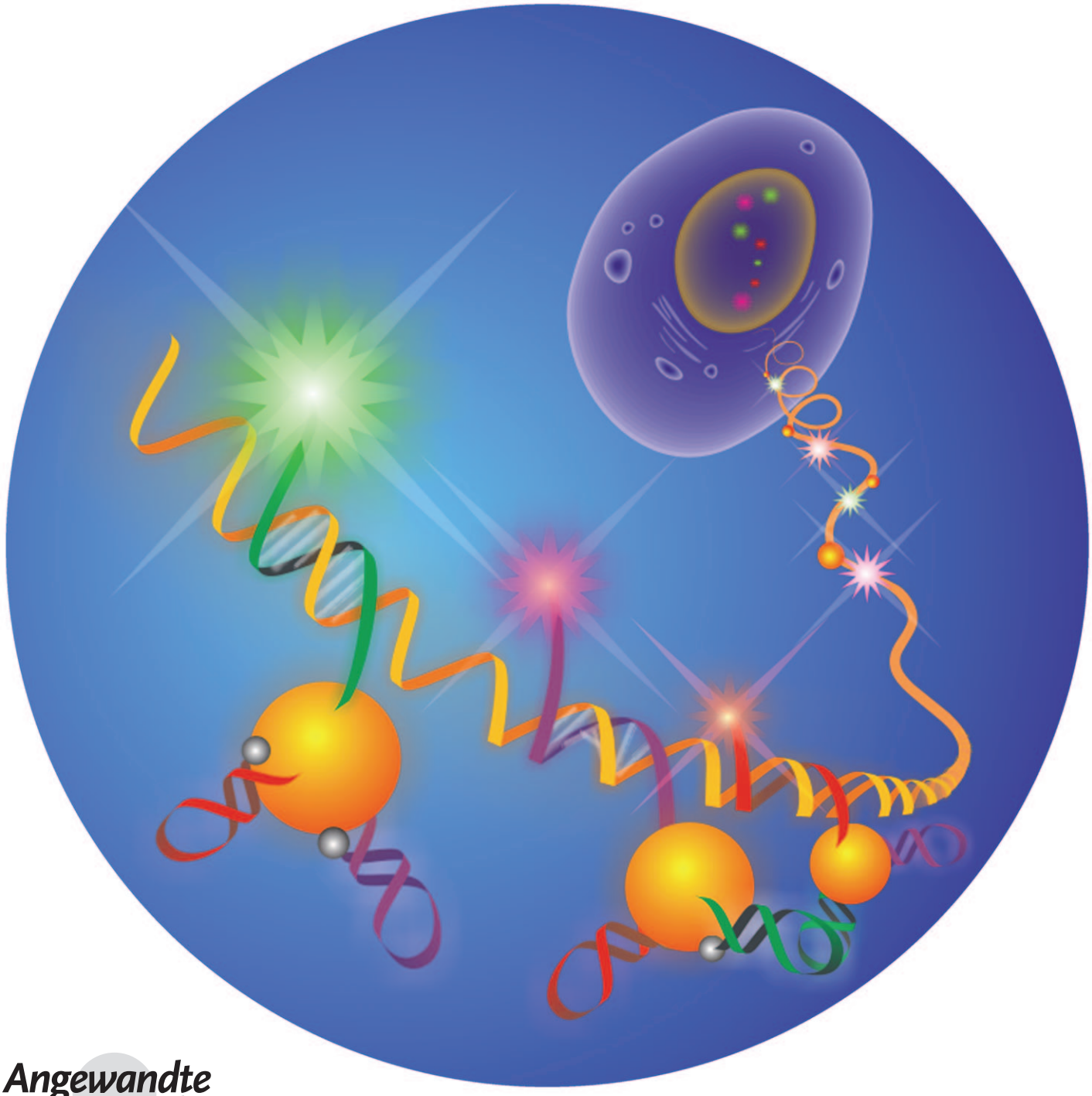

There has been ever-increasing demand to develop rapid, sensitive, and selective bioassay methods in various areas including molecular diagnostics, environmental monitoring, and civil defense.[1–6] A particularly attractive molecular tool toward this goal is the molecular beacon (MB).[7–12] MBs are dually labeled, stem–loop-structured oligonucleotides that are internally quenched as a result of the close contact between a dye–quencher pair (e.g., tetramethyl-6-carboxyrhodamine (TAMRA) and 4-{[4′-(dimethylamino)phenyl]azo}benzoic acid (DABCYL)) attached at either end.[7] Target binding in the loop (probe) region competitively opens the stem–loop structure and forces apart the dye and the quencher, which turns on fluorescence that signals the presence of a complementary target sequence.[7,9] MBs possess several combined advantages, such as signal-on sensing and high sequence specificity resulting from the conformational constraint offered by the stem–loop structure.[13] Because of these unprecedented merits, MBs have found wide applications in molecular and cellular biology, pathogen detection, and biomedical diagnostics.[8,10]

Since their original design, MBs have been refined in various aspects. The choice of quenchers is of particular interest as it may lead to higher quenching efficiency and a lower "OFF" signal. Notably, although traditional organic quenchers have proven effective to quench the fluorescence of given fluorophores located in their proximity, their quenching efficiencies usually vary significantly from one dye to another.[9,11] For example, DABCYL efficiently quenches the fluorescence of fluorescein (FAM), but is much less efficient for dyes emitting at longer wavelengths (e.g., Texas red and the cyanine dye Cy5).

Metallic gold (macroscopic gold and gold nanoparticles, AuNPs) is well known for its ultrahigh fluorescence quenching ability as theoretically predicted and experimentally observed.[14–17] Indeed, Krauss and co-workers reported a surface-confined MB by using macroscopic gold films.[18–20] Dubertret et al. constructed the first AuNP-based MB by attaching a fluorophore-tagged stem–loop probe at the surface of small AuNPs (1.4 nm),[11] which led to high quenching efficiencies toward a range of organic fluorophores. Maxwell et al. reported a different design that employed a dye-tagged linear oligonucleotide (stemless probe) that curved at the 2.5 nm AuNP surface because of the strong dye–AuNP adsorption.[21]

Herein, we report the use of relatively large AuNPs (15 nm) to construct multicolor nanoscale MBs (nanoMBs). Such large-sized AuNPs possess strong surface plasmon resonance (SPR) absorption which exceeds that of 1 or 2 nm AuNPs by orders of magnitude.[16] More importantly, small-sized AuNPs can only accommodate one or several oligonucleotides,[21] whereas the use of large AuNPs allows the anchoring of many oligonucleotides at a single particle, thus providing the opportunity to construct multicolor nanoMBs. Initially, we prepared nanoMBs by following the classic self-assembly approaches developed by Mirkin and others.[22–27] That is, a stem–loop oligonucleotide dually labeled with FAM and thiol was incubated with AuNPs, allowed to self-assemble through the Au–S bond, and then "aged" in salt solution.[23] However, we found that such a AuNP–DNA conjugate turned from red to blue during the aging step, a phenomenon suggesting the formation of large aggregates.[23] We ascribe this effect to the low surface density of AuNPs modified with stem–loop structures.

AuNPs heavily loaded with linear DNA strands possess strong interparticle electrostatic repulsion (Figure 1 A), which protects the AuNPs from being aggregated in salt solution.[23,28] However, since stem–loop structures are formed in buffer before self-assembly, the presence of bulky structures significantly lowers the surface density at the AuNPs (Figure 1 B), which leads to unstable AuNP–DNA conjugates. It is also possible that bulky structures lead to steric stabilization of AuNPs. While this possibility cannot be excluded, our experimental observation suggests that this effect plays a smaller role. Notably, the 1 nm AuNPs employed in the previous report were extensively coated before conjugation

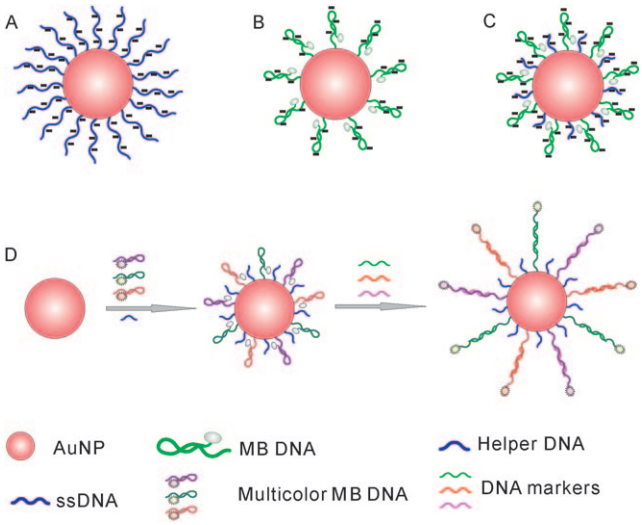

Figure 1. Assembly of nanoMBs: A) AuNPs self-assembled with densely loaded linear probes (stable nanoparticles); B) AuNPs self-assembled with sparsely loaded stem–loop probes (easily aggregated); C) AuNPs self-assembled with stem–loop probes and helper oligonucleotides (stable nanoMBs); D) AuNPs self-assembled with multicolor stem–loop probes and helper oligonucleotides (stable multicolor nanoMBs). ssDNA = single-stranded DNA.

[*] Prof. S. Song, Dr. Z. Liang, J. Zhang, Dr. L. Wang, Prof. C. Fan
Laboratory of Physical Biology, Shanghai Institute of Applied Physics, Chinese Academy of Sciences, Shanghai 201800 (China)
Fax: (+86) 21-5955-6902
E-mail: fchh@sinap.ac.cn
Prof. G. Li
Department of Biochemistry and State Key Laboratory of Pharmaceutical Biotechnology, Nanjing University
Nanjing 210093 (China)
E-mail: genxili@nju.edu.cn

[**] This work was supported by the National Natural Science Foundation (20725516, 20873175, 60537030), Ministry of Science and Technology (2006CB933000, 2007CB936000, 2007AA06A406), Ministry of Health (2009ZX10004-301), and Shanghai Municipal Commission for Science and Technology (0952nm04600, 08jc1422600).

Supporting information for this article is available on the WWW under http://dx.doi.org/10.1002/anie.200901887.

with oligonucleotides,[11] which is fundamentally different from the 15 nm AuNPs employed in this work.

We then modified the original assembly protocol with the introduction of short "helper" oligonucleotides, that is, 3′-thiolated oligo-Ts (10 Ts). The oligo-Ts were co-assembled with the stem–loop oligonucleotide to form a mixed monolayer at the surface of the AuNPs (Figure 1 C). We expect that these short oligonucleotides form a dense layer at the nanoparticle surface, which protects the AuNPs from being aggregated during the aging step. Indeed, the employment of the helper oligonucleotides significantly increased the stability of the nanoMBs, which remained dispersed (characterized by the red color) even at high ionic strength (e.g., 1 M NaCl). Also of note, the stem–loop oligonucleotide (35 base) employed in this work is appended with a 10-T spacer at the 3′ end; thus, the presence of helper strands of equivalent length does not sterically prevent the formation of the stem–loop structure.[28]

The performance of nanoMBs is critically dependent on the ratio between the probe and the helper oligonucleotides in the assembly solution. Indeed, nanoMBs were not stabilized at low ratio (e.g., 1:10), which still resulted in the aggregation of the nanoparticles. On the other hand, although nanoMBs were successfully prepared at high ratio (e.g., 10:1), the signal of the nanoMBs at the "ON" state was low because of the very low surface density of the stem–loop probe (data not shown). We experimentally chose a ratio of 2:1 for the preparation of nanoMBs, which provides a trade-off between the stabilization and the signal intensity. By following a well-established displacement-based fluorescence assay protocol,[28] we found that each nanoMB (15 nm AuNPs) carried approximately 40–50 strands (44 ± 5) of probe DNA.

Similar to MBs, nanoMBs stay in the "close" state in the absence of targets but fluoresce when they meet the specific target. Indeed, we found that nanoMBs responded rapidly to DNA of the complementary sequence (cDNA), with fluorescence recovery of up to 90% within 5 min (Figure 2 A). This kinetics is apparently much faster than that of the previously reported stemless AuNP-based MBs (ca. 40% within 5 min),[21] but similar to that of conventional solution-phase stem–loop MBs.[7] This is possibly because the use of the 10-T spacer and the stem makes the surface-attached probes more hybridizable than the stemless probes previously employed.[21]

We examined the sequence discrimination ability of nanoMBs toward single-base-mismatched DNA. Importantly, target DNA with one mismatch led to only about 50% of the fluorescence of the complementary DNA. This difference demonstrates that nanoMBs retain the high sequence specificity offered by the conformational constraint of stem–loop structures.[13] We then investigated the thermodynamics of nanoMBs by monitoring the fluorescence change in the absence and presence of targets over a temperature profile. Interestingly, the thermodynamic behavior of nanoMBs closely resembles that of conventional MBs (Figure 2 B).[13] In the absence of targets, nanoMBs are held in the "close" state with minimal fluorescence at low temperature. Then the fluorescence is gradually turned on along with the temperature elevation and resulting thermal destabilization of the stem–loop structure that separates the dye and AuNPs. In the presence of target DNA, nanoMBs exhibit a characteristic MB-like three-state behavior. Initially, nanoMBs are fluorescent at low temperature as a result of the formation of a duplex in the loop region and the opening of the hairpin stem (Phase I). As the temperature exceeds 36 °C, the probe–target duplex is dehybridized, and the re-formation of the hairpin holds the dye in the proximity of the AuNPs, which leads to a decrease of the fluorescence (Phase II). In the third phase, the fluorescence again increases because the stem–loop structure melts into extended random coils at temperatures over 54 °C (Phase III).

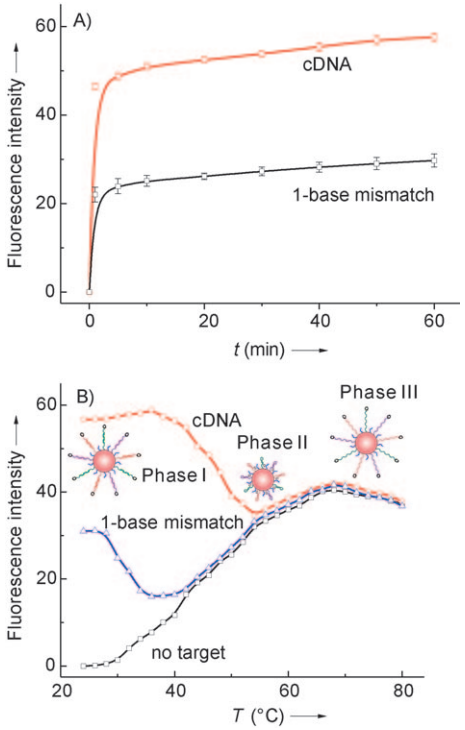

Figure 2. Kinetic and thermodynamic studies of nanoMBs. A) Kinetics of nanoMBs in response to a perfectly matched target (red curve: 5′-GGAATAATAATAAGG-3′) and single-base-mismatched DNA (black curve: 5′-GGAATAACAATAAGG-3′). B) Variation of the fluorescence intensity of nanoMBs over a temperature profile in the presence of perfectly matched target or single-base-mismatched DNA, as well as in the target-free condition. The shown structures demonstrate the conformational change of surface-attached probes during the phase transitions.

We further interrogated the interaction of nanoMBs with a single-base-mismatched DNA. We observed a similar temperature-variation-induced three-state phase transition; however, significantly, the two phase transitions occur at much lower temperatures (27 and 37 °C, respectively). This difference in the phase transition reflects the lowered thermodynamic stability because of the incorporation of one mismatch, which provides a powerful means to conveniently discriminate single mismatches.[7,9,13] For example, the fluorescence of the complementary DNA is about twofold that of single-base-mismatched DNA at room temperature (Figure 2 B), but about fourfold at 36 °C. Overall, the similarity of nanoMBs to MBs in their thermodynamics

suggests that the stem–loop oligonucleotides retain their constrained conformation at the nanoparticle surface, and this constraint similarly offers an enhanced sequence specificity over linear probes.[13]

It is important to detect multiple targets in a variety of applications. For example, cancers are often associated with multiple tumor DNA markers (e.g., tumor-suppressor genes) that have proven valuable for the early-phase detection of cancers in asymptomatic individuals.[29] Toward this goal, Tyagi and co-workers designed a series of multicolor MBs, each with emitting light of a different color.[9] Given that each AuNP carries about 44 stem–loop probes, we reason that multiple MBs with different colors might be integrated into individual AuNPs. We constructed multicolor nanoMBs by assembling multiple hairpin probes labeled with different fluorophores on the surface of AuNPs (Figure 1D). Three probes targeting three types of tumor-suppressor genes (exon segments of p16, p21, and p53 genes) were employed, which were labeled with FAM, Cy5, and Rox, respectively. Hybridization tests were carried out with solutions spiked with a mixture of three targets. Interestingly, the nanoMBs respond only to the specific target, and signal characteristic colors with negligible crosstalk. That is, P16 produces a blue color corresponding to the emission of FAM, P21 produces a red color corresponding to the emission of Cy5, and P53 produces an orange color corresponding to the emission of FAM.

As shown in Figure 3, the fluorescence of the nanoMBs increases along with the concentration of each target over the concentration range from 500 pM to 200 nM. Significantly, the multicolor nanoMBs retain the high sequence specificity that arises from the conformational constraint. We interrogated three targets carrying single mismatches, and all responded with significantly lower fluorescence over the examined concentration profile (Figure 3). These data suggest that nanoMBs can not only recognize specific gene targets, but also might be appropriate for more challenging applications such as allele discrimination.

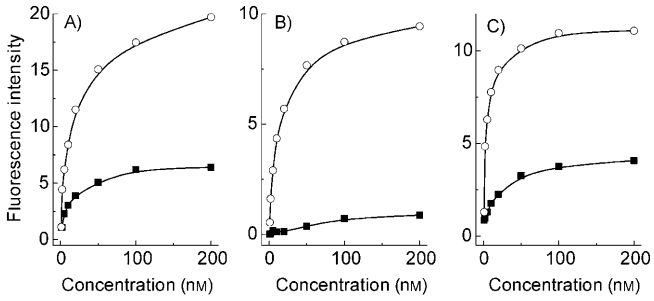

Figure 3. Multiplexing detection using multicolor nanoMBs. The multicolor nanoMBs (0.5 nM) are hybridized with three perfectly matched targets (○) and three single-mismatched targets (■); target concentrations range from 500 pM to 200 nM. A) P16 gene (FAM, blue emission at 520 nm); B) P21 gene (Cy5, red emission at 667 nm); C) P53 gene (Rox, orange emission at 607 nm).

In summary, we have reported the design of nanoMBs that rapidly respond to DNA targets in a mix-and-detect way. Dually labeled hairpin probes (thiol and dye) are assembled at the surface of AuNPs through the Au–S bond. The dye is held in the proximity of the AuNPs because of the formation of the stem, which results in efficient gold-quenched fluorescence ("close" state). In the presence of the target, duplex formation between the probe and the target competitively unzips the stem and restores the fluorescence as a result of the separation of the dye from the AuNPs.

The nanoMBs combine the advantages of MBs with the superior properties of AuNPs. First, since gold is a highly efficient quencher for almost all fluorophores, this configuration serves as a universal beacon design without the necessity to optimize the fluorophore–quencher pair. Moreover, there is an additional decay channel for nonradiative energy transfer from the dye to large-sized AuNPs, which potentially means that the use of large AuNPs enhances fluorophore quenching.[17] Second, the nanoMBs display similar thermodynamic behavior to conventional solution-phase MBs. Analogously, nanoMBs possess high sequence specificity toward single-mismatch discrimination because of the conformation constraint of the stem–loop structure. Third, in contrast to the previously employed small-sized AuNPs,[11,21] the increased surface area of large AuNPs allows the accommodation of many probes on one particle, thus providing the opportunity to design all-in-one multicolor nanoMBs. Although we only demonstrate a three-color nanoMB with 15 nm AuNPs, we reason that nanoMBs incorporating more fluorophores might be synthesized with larger AuNPs. Fourth, this strategy can be easily extended to designing aptamer-based nanoprobes for the simultaneous multianalysis of various protein and small-molecule analytes.[30–33] Fifth, given that AuNP–DNA conjugates show highly efficient cellular uptake, it is possible to develop intracellular nanoprobes that signal cellular events in real time.[34]

Received: April 8, 2009
Revised: June 17, 2009
Published online: September 3, 2009

Keywords: DNA · fluorescent probes · gold · molecular beacons · nanoparticles

[1] M. J. Heller, *Annu. Rev. Biomed. Eng.* **2002**, *4*, 129.
[2] R. C. McGlennen, *Clin. Chem.* **2001**, *47*, 393.
[3] E. Katz, I. Willner, *Angew. Chem.* **2004**, *116*, 6166; *Angew. Chem. Int. Ed.* **2004**, *43*, 6042.
[4] U. Feldkamp, C. M. Niemeyer, *Angew. Chem.* **2006**, *118*, 1888; *Angew. Chem. Int. Ed.* **2006**, *45*, 1856.
[5] Y. Cui, Q. Wei, H. Park, C. M. Lieber, *Science* **2001**, *293*, 1289.
[6] C. Fan, K. W. Plaxco, A. J. Heeger, *Proc. Natl. Acad. Sci. USA* **2003**, *100*, 9134.
[7] S. Tyagi, F. R. Kramer, *Nat. Biotechnol.* **1996**, *14*, 303.
[8] W. Tan, K. Wang, T. J. Drake, *Curr. Opin. Chem. Biol.* **2004**, *8*, 547.
[9] S. Tyagi, D. P. Bratu, F. R. Kramer, *Nat. Biotechnol.* **1998**, *16*, 49.
[10] K. Wang, Z. Tang, C. J. Yang, Y. Kim, X. Fang, W. Li, Y. Wu, C. D. Medley, Z. Cao, J. Li, P. Colon, H. Lin, W. Tan, *Angew. Chem.* **2009**, *121*, 870; *Angew. Chem. Int. Ed.* **2009**, *48*, 856.
[11] B. Dubertret, M. Calame, A. J. Libchaber, *Nat. Biotechnol.* **2001**, *19*, 365.
[12] N. E. Broude, *Trends Biotechnol.* **2002**, *20*, 249.

[13] G. Bonnet, S. Tyagi, A. Libchaber, F. R. Kramer, *Proc. Natl. Acad. Sci. USA* **1999**, *96*, 6171.
[14] P. C. Das, A. Puri, *Phys. Rev. B* **2002**, *65*, 155416.
[15] E. Dulkeith, A. C. Morteani, T. Niedereichholz, T. A. Klar, J. Feldmann, S. A. Levi, F. C. van Veggel, D. N. Reinhoudt, M. Moller, D. I. Gittins, *Phys. Rev. Lett.* **2002**, *89*, 203002.
[16] C. Fan, S. Wang, J. W. Hong, G. C. Bazan, K. W. Plaxco, A. J. Heeger, *Proc. Natl. Acad. Sci. USA* **2003**, *100*, 6297.
[17] E. Dulkeith, M. Ringler, T. A. Klar, J. Feldmann, A. Munoz Javier, W. J. Parak, *Nano Lett.* **2005**, *5*, 585.
[18] H. Du, M. D. Disney, B. L. Miller, T. D. Krauss, *J. Am. Chem. Soc.* **2003**, *125*, 4012.
[19] H. Du, C. M. Strohsahl, J. Camera, B. L. Miller, T. D. Krauss, *J. Am. Chem. Soc.* **2005**, *127*, 7932.
[20] C. M. Strohsahl, B. L. Miller, T. D. Krauss, *Nat. Protoc.* **2007**, *2*, 2105.
[21] D. J. Maxwell, J. R. Taylor, S. Nie, *J. Am. Chem. Soc.* **2002**, *124*, 9606.
[22] C. A. Mirkin, R. L. Letsinger, R. C. Mucic, J. J. Storhoff, *Nature* **1996**, *382*, 607.
[23] R. Elghanian, J. J. Storhoff, R. C. Mucic, R. L. Letsinger, C. A. Mirkin, *Science* **1997**, *277*, 1078.
[24] J. Liu, Y. Lu, *Nat. Protoc.* **2006**, *1*, 246.
[25] J. Zhang, S. P. Song, L. H. Wang, D. Pan, C. Fan, *Nat. Protoc.* **2007**, *2*, 2888.
[26] S. J. Park, T. A. Taton, C. A. Mirkin, *Science* **2002**, *295*, 1503.
[27] J. Zhang, S. Song, L. Zhang, L. Wang, H. Wu, D. Pan, C. Fan, *J. Am. Chem. Soc.* **2006**, *128*, 8575.
[28] L. M. Demers, C. A. Mirkin, R. C. Mucic, R. A. Reynolds, R. L. Letsinger, R. Elghanian, G. Viswanadham, *Anal. Chem.* **2000**, *72*, 5535.
[29] D. Sidransky, *Science* **1997**, *278*, 1054.
[30] A. D. Ellington, J. W. Szostak, *Nature* **1990**, *346*, 818.
[31] S. Song, L. Wang, J. Li, J. Zhao, C. Fan, *TrAC Trends Anal. Chem.* **2008**, *27*, 108.
[32] J. W. Liu, Y. Lu, *Angew. Chem.* **2006**, *118*, 96; *Angew. Chem. Int. Ed.* **2006**, *45*, 90.
[33] T. Hermann, D. J. Patel, *Science* **2000**, *287*, 820.
[34] N. L. Rosi, D. A. Giljohann, C. S. Thaxton, A. K. R. Lytton-Jean, M. S. Han, C. A. Mirkin, *Science* **2006**, *312*, 1027.

